Available online at www.sciencedirect.com
ScienceDirect
Photonics and Nanostructures – Fundamentals and Applications xxx (2014) xxx–xxx
PHOTONICS AND NANOSTRUCTURES Fundamentals and Applications
www.elsevier.com/locate/photonics

Bandwidth and gain enhancement of optically transparent 60-GHz CPW-fed antenna by using BSIS-UC-EBG structure

Ning Wang, Huiping Tian *, Zheng Guo, Daquan Yang, Jian Zhou, Yuefeng Ji

The State Key Laboratory of Information Photonics and Optical Communications, School of Information and Communication Engineering, Beijing University of Posts and Telecommunications, Beijing 100876, China

Received 30 September 2014; received in revised form 18 November 2014; accepted 24 November 2014

Abstract

A method in terms of bandwidth and gain enhancement is presented for optically transparent coplanar waveguide fed (CPW-Fed) antenna, which supports unlicensed 60 GHz band (57–66 GHz) applications. The original antenna and mesh antenna in [8] were designed on a transparent material that is made of a 0.2-mm-thick fused silica 7980 Corning substrate (ε_r: 3.8 and tan δ: 0.0001). However, the peak gains of −5.3 and −5.4 dBi at 60 GHz of those antennas can be further improved. Thus, in this paper, a novel bidirectional symmetric I-shaped slot uniplanar compact electromagnetic band-gap (BSIS-UC-EBG) structure with a reflection phase band of 58.0–62.1 GHz is proposed to improve antenna performance. Based on this BSIS-UC-EBG structure, both transparent BSIS-UC-EBG antenna and transparent mesh BSIS-UC-EBG antenna with enhanced properties are presented and discussed. The analysis results show that the impedance bandwidth (the peak gain) of transparent BSIS-UC-EBG antenna and transparent mesh BSIS-UC-EBG antenna are enhanced to 36.6% (4.7 dBi) and 44.7% (5.8 dBi), respectively. In addition, we also discuss the comparison of radiation patterns at 60 GHz, and the results illustrate that the radiation patterns are basically identical.

Keywords: 60 GHz; BSIS-UC-EBG; Transparent mesh antenna; High gain; Wideband

1. Introduction

As wireless communications have been generally studied and dramatically promoted in the past few decades, applications involving Wireless Personal Area Network (WPAN), vehicular and navigation communications make new demands for conformal and optically transparent antennas. These antennas can be installed on building windows, light panels, monitors of mobile devices, windshields of vehicles or vessels, to realize enhanced performance, security and esthetics purposes. The first feasibility study of optically transparent antenna was conducted by National Aeronautics and Space Administration (NASA) Lewis Research Center Nyma Group [1]. They proposed two antennas with AgHT-8 optically transparent conductive coating deposited on sheets of clear polyester which operate at 2.3 and 19.5 GHz, respectively. Radiation patterns were studied and had good match with conventional opaque antennas. In Ref. [2], optically transparent antennas made from five different kinds of materials were fabricated and measured. Conventional copper-based antennas were also used as references. The author demonstrated that

* Corresponding author at: Beijing University of Posts and Telecommunications, P.O. Box 90, #10 Xitucheng Road, Haidian District, Beijing 100876, China. Tel.: +86 10 62282153.
E-mail address: hptian@bupt.edu.cn (H. Tian).

http://dx.doi.org/10.1016/j.photonics.2014.11.002
1569-4410/© 2014 Published by Elsevier B.V.

transparent coating like gold (Au) and silver (Ag) could be good candidates for transparent antennas. Beyond that, Colombel et al. [3] investigated multilayer technology for UHF band transparent antennas, drawing the conclusion that ITO/Cu/ITO could be the trade-off between transparency and radio-electrical properties. Most of previously proposed transparent monopole antennas could be built from conductive and transparent coating deposited on see-through substrates [4–8] by radio frequency sputtering (RF sputtering is the technology that uses positive ion in radio frequency discharge plasma to bombard the target, sputter target atoms, and deposit them on the grounding surface of the substrate). Radio-electrical performances and transparency of all mentioned antennas were discussed, validating the feasibility of the proposed designs.

Recent researches adopt Ag/Ti bilayer with mesh structures printed on it by standard photolithographic wet etching process [6,7], and attain properties close to analogous non-transparent antennas. Nevertheless, most of the above transparent antennas operated at low frequencies. For instance, antennas working at 800 MHz [2,3,6], 2.4 GHz [4], 19.5 GHz [1], and 1–6 GHz [5] were reported, respectively. As a hotspot in modern communication technologies, the unlicensed 60 GHz band bears 9 GHz bandwidth and gigabits data rates. Consequently, millimeter-wave antenna featuring good bandwidth and gain performance is in demand for current wireless communication. Hautcoeur et al. [8] conducted a study on optically transparent monopole antenna operating at 60 GHz.

With current tendency for wideband and high gain antennas [9], periodic electromagnetic structures, which have the same characteristics with frequency selective surface (FSS) and high-impedance surface (HIS), have been a good candidate to optimize the antenna performance. They are usually viewed as artificial magnetic conductor (AMC) or electromagnetic band-gap (EBG) structure. Extensive researches on improving antenna performance by introducing periodic structures have been done in recent past [10]. In Ref. [11], the Spiral-arms-shaped metallo-electronic band-gap structure (MEBG) was embedded in a ultra-wide bandwidth (UWB) monopole antenna for achieving an impedance bandwidth of 33 GHz, with a 60% reduction in antenna size. Beyond that, the stop band property of mushroom-like EBG structures could also be used to design the trap UWB antenna [12], broaden bandwidth of microstrip antenna [13] and improve antenna's gain and directivity performance [14]. Using the presented aperture-coupled microstrip patch antenna (ACMPA) in [15] as a reference, a 16-element array of uniplanar-compact EBG structure was designed and loaded around the radiating patch, with a 4.5 dBi gain increase. It was also proved that UC-EBG surface could reduce the E-plane coupling in the 16 element patch array by 11 dB [16]. Mushroom-like EBG could reduce mutual coupling of surface waves in aperture coupled microstrip antenna [17] and waveguide-slot-array antennas [18]. In addition to that, the HIS which is organized by quasi-periodic structures had been proposed, with the ability to control the phase of radiated field or scattered field [19]. Design methodology of compact miniaturized EBG structures was studied and applied to achieve reduction in antenna electrical size [20].

The periodic electromagnetic structures can have different functions corresponding to different locations in antennas. The Sievenpiper EBG, which locates on the top three layers of LTCC tape, can realize a 6 dB enhancement in antenna's broadside directivity performance by preventing the main beam been degraded into two lobes [21]. Superstrate consisted of EBG could be reflective surface and form a resonant cavity with metallic ground plane, resulting in antenna gain enhancement [22]. In Ref. [23], a dual-layer FSS, which is placed under the antenna, achieved an ultra-wide in phase reflection band, and dramatically improved the antenna gain. The FSS could not only play the role of shield between antenna and conducting surfaces, but also prevent impedance mismatch in antenna [24]. Thus, the thought of presenting a 60 GHz transparent periodic electromagnetic structure to improve the performance of transparent antenna and transparent mesh antenna, which have not been studied before, naturally came to the authors' mind.

The aim of this paper is to deliver the feasibility for promoting properties of optically transparent antennas with BSIS-UC-EBG (Bidirectional symmetrical I-shaped slot uniplanar-compact Electromagnetic Band-gap), and to present potentially an ideal transparency components which can be used for wireless communications.

This paper is structured as follows. In Section 2, two structures of EBGs and optically transparent antennas loaded with EBG are thoroughly elaborated. And the design philosophy of transparent antennas is also introduced in this section. Then, in Section 3, we discuss the analysis results of former structures presented in Section 2. The detailed optimization process and reflection phase curves of EBG have been shown to justify the rationality of the BSIS-UC-EBG. Antennas' performances on impedance bandwidth, gain and radiation pattern have also been discussed. Finally, Section 4 draws the conclusion.

Please cite this article in press as: N. Wang, et al. Bandwidth and gain enhancement of optically transparent 60-GHz CPW-fed antenna by using BSIS-UC-EBG structure, Photon Nanostruct: Fundam Appl (2014), http://dx.doi.org/10.1016/j.photonics.2014.11.002

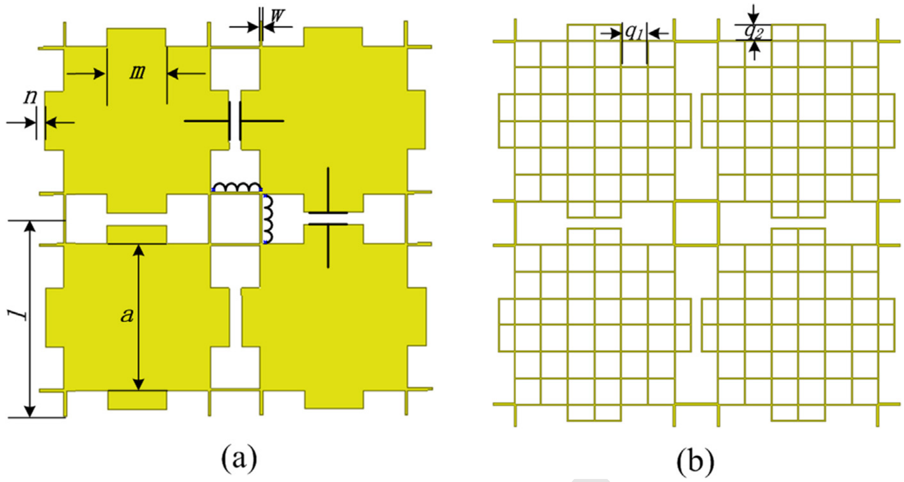

Fig. 1. A sketch of frequency selective surface consists of (a) transparent BSIS-UC-EBG cells and (b) mesh BSIS-UC-EBGs.

2. Geometry and designs

2.1. Configurations of EBGs

The configuration of BSIS-UC-EBG is shown in Fig. 1(a), which is designed for millimeter-wave application on a fused silica 7980 Corning substrate with thickness of 0.2 mm, $\varepsilon_r = 3.8$ and tan $\delta = 0.0001$. There are four half-I slots on each side of EBG cell, and four squares slots on corners. The period of the BSIS-UC-EBG cell is denoted by l. A uniformly distributed pattern of periodical EBG cells forms frequency selective surface (FSS), and the equivalent impedance of the grid is constituted by multiple inductors and capacitors [11], which can be expressed as:

$$Z = \frac{\eta^2}{4} \times \frac{j\omega C}{1 - \omega^2 LC} \tag{1}$$

where η denotes the effective wave impedance (η_0 is free-space impedance) and can be calculated by formula $\eta = 2\eta_0/(\varepsilon_r + 1)$, ε_r is the dielectric constant of dielectric sheet [11]. Periodic BSIS-UC-EBG distribution can be equivalent to LC resonant circuit, with inductance formed at the joints of adjacent cells and conductance formed by gaps between cells. Since $C = \varepsilon S/4\pi kd$, the main capacitors are constructed by the gaps whose $d = 2 \times n$, which is shown in Fig. 1(a). According to $f_r = 1/(2\pi\sqrt{LC})$, resonant frequency of the EBG structure is tuned to 60 GHz, with corresponding detailed sizes listed in Table 1. Theoretically, the BSIS-UC-EBG, which is frequency-dependent, has great influence on antenna radiating at resonant frequency. A small effect from EBG to the radiating patch can be made when frequency is below the resonance. However, as resonant frequency dominants the operation, the BSIS-UC-EBG becomes radiating structure itself with large currents induced, resulting in gain improvement. TM surface wave will be blocked by EBG when frequency is above resonance. Thus, EBG can be used to obtain a higher antenna gain when properly designed.

To improve the antenna performance with higher transparency level of the whole structure, mesh BSIS-UC-EBG with the identical overall dimensions of 1.6 mm × 1.6 mm is designed. Considering availability of the mesh design for 60 GHz antenna, physical dimensions are optimized using the simulation software High Frequency Structure Simulator (HFSS). As is depicted by Fig. 1(b), the width of strips forming inductance equals to the original size (0.02 mm), while other strips have the width of 0.01 mm, which has been adjusted to form the same resonant frequency with transparent ones. The pitch of the grid (q_1) equals to 0.2 mm, and the half-grid has a height (q_2) of 0.15 mm.

2.2. Structures of optically transparent antennas with EBGs

Recent researches on optically transparent antennas employed the design philosophies that mesh conductor acted as radiator and that optical or electrical signals travel through the mesh openings [8]. The material

Table 1
The dimensions of BSIS-UC-EBG.

Parameters	l	w	a	n	m	q_1	q_2
Unit (mm)	1.6	0.02	1.2	0.04	0.48	0.2	0.15

Please cite this article in press as: N. Wang, et al. Bandwidth and gain enhancement of optically transparent 60-GHz CPW-fed antenna by using BSIS-UC-EBG structure, Photon Nanostruct: Fundam Appl (2014), http://dx.doi.org/10.1016/j.photonics.2014.11.002

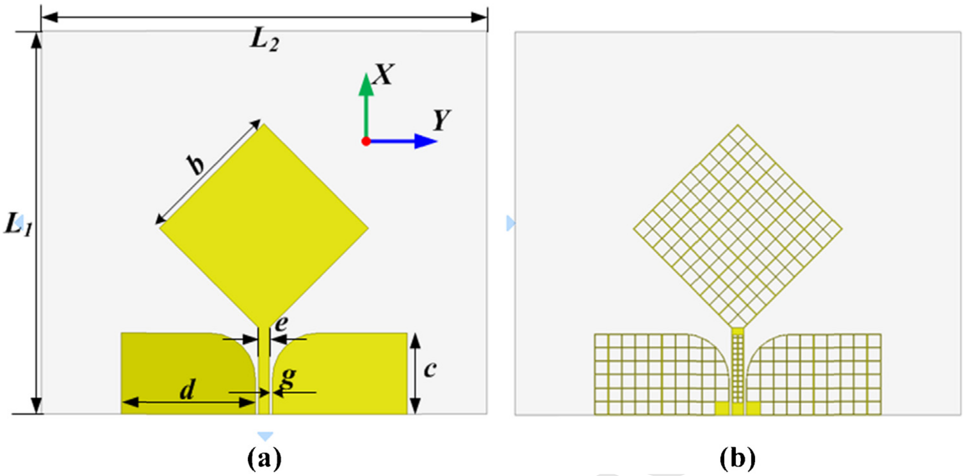

Fig. 2. (a) Transparent antenna and (b) transparent mesh antenna on fused silica 7980 Corning substrates.

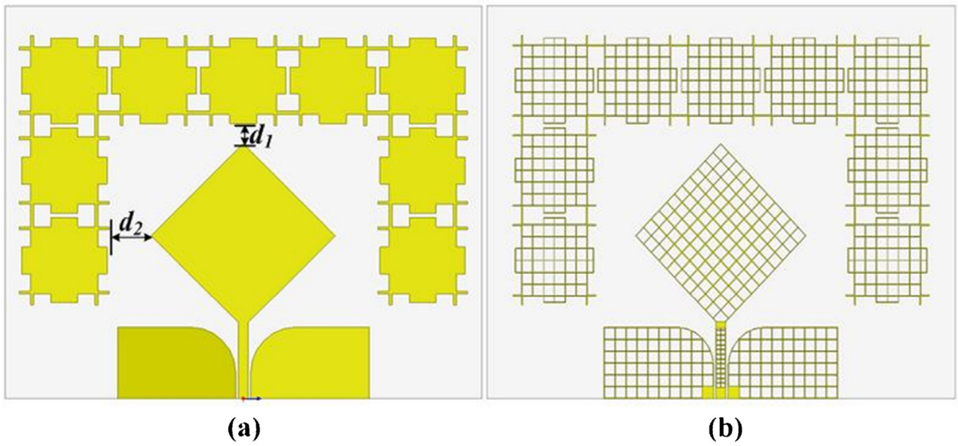

Fig. 3. The layout of (a) transparent BSIS-UC-EBG antenna and (b) transparent mesh BSIS-UC-EBG antenna.

usually used to form conductive film is silver grid layer (AgGL) in [6] (with a 6-μm thick silver film and a 5 nm titanium (Ti) layer printed on a 1737 Corning glass), AgHT in [5], and gold grid layer (AuGL) in [8]. Ohmic loss and skin depth loss from conductive material are two main influence factors which need to be concerned. Theoretically, the material with lower sheet resistance R_s and higher thickness can have best radiation efficiency, because ohmic loss decreases with sheet resistance going down and skin depth loss increases when metal thickness decreases. According

Table 2
The dimensions of transparent antenna.

Parameters	L_1	L_2	b	c	d	e	g
Unit (mm)	7	9	2.32	1.27	2.11	0.18	0.045

to Ref. [3], a formula between sheet resistance and thickness can be expressed as follows:

$$R_s = \frac{\rho}{d} \quad (2)$$

where ρ represents the resistivity of selected material. Skin depth δ is expressed as

$$\delta = \sqrt{\frac{2}{\mu_0 \omega \sigma}} \quad (3)$$

where μ_0 represents the permeability of free space, ω is angular frequency and σ is the conductivity of the conductive layer. With the design principle that skin depth loss can be limited by a metallic layer 2 times thicker than the skin depth, a 0.93-μm-thick gold (Au) layer is used as a replacement for silver (Ag) layer, and the first optically transparent antenna for 60 GHz applications is proposed by Hautcoeur et al. [8]. A 10 nm-thick titanium

Please cite this article in press as: N. Wang, et al. Bandwidth and gain enhancement of optically transparent 60-GHz CPW-fed antenna by using BSIS-UC-EBG structure, Photon Nanostruct: Fundam Appl (2014), http://dx.doi.org/10.1016/j.photonics.2014.11.002

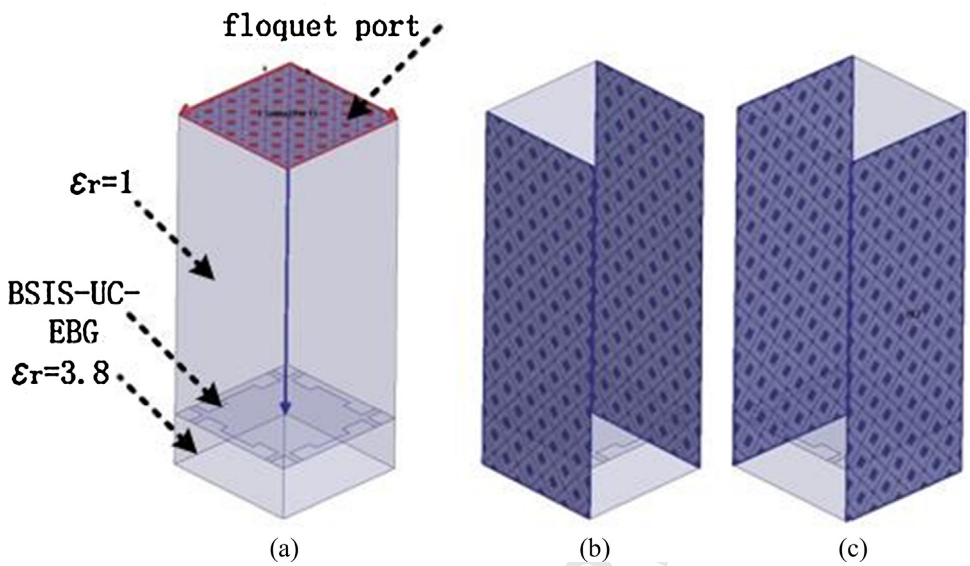

Fig. 4. The HFSS simulation model for a BSIS-UC-EBG cell. (a) The geometry and the *Floquet-port* excitation; (b) *Perfect-E* symmetry planes; (c) *Perfect-H* symmetry planes.

(Ti) layer and the gold metallization are deposited on a fused silica 7980 Corning substrate with thickness of 0.2 mm, $\varepsilon_r = 3.8$ and tan $\delta = 0.0001$. A transparent monopole lozenge antenna was designed in [8], which is also the design prototype of our research, is studied as a reference to the mesh antenna. Fig. 2 shows the configurations of transparent antenna and transparent mesh antenna. Sizes of transparent antenna have been optimized in this article to get better performances, resulting in the definite dimensions illustrated in Table 2. The grid inner side width of transparent mesh antenna is 0.2 mm, with a gold strip width of 10 μm. The pitch of feeding line is set as 100 μm to lower sheet resistance.

A period of BSIS-UC-EBG cells is placed around the lozenge radiating patch on top side of the Corning substrate, as shown in Fig. 3. To make patch radiation avoid from being distorted by loaded structure, the distances from BSIS-UC-EBGs to patch edges are optimized using HFSS and result in $d_1 = 0.32$ mm and $d_2 = 0.76$ mm. The transparent mesh BSIS-UC-EBG antenna, which has the same layout and material with transparent BSIS-UC-EBG antenna, can be manufactured by sputtering and photolithographic. Square apertures periodically distributed can be obtained by the stripping of photoresist.

3. Results and discussion

To attain the optimal performances of the BSIS-UC-EBG and antenna loaded with EBG, the HFSS software is applied to conduct the optimization design. Firstly, a parametric analysis process is performed to confirm accurate dimensions of EBG. Both the reflection phase curves of the transparent BSIS-UC-EBG and transparent mesh BSIS-UC-EBG are graphed and analyzed. Then impedance bandwidth and gain properties of four mentioned antennas are depicted and discussed. Finally, radiation patterns of two antennas are demonstrated.

3.1. Parametric study of BSIS-UC-EBG

As the simulation model depicted in Fig. 4, the BSIS-UC-EBG unit cell is deposited on the top side of a $1.6 \times 1.6 \times 0.2\,\text{mm}^3$ fused silica 7980 Corning substrate ($\varepsilon_r = 3.8$, $\tan\delta = 0.0001$), with symmetrical *perfect-E* and *perfect-H* planes imitating infinite distribution of periodic BSIS-UC-EBG. A *Floquet port* is placed on the position of 1.2 mm above the EBG surface and de-embedded the same distance into the simulation model. Fig. 5 illustrates the parametric analysis of BSIS-UC-EBG in terms of reflection phase. Fig. 5(a) shows the results of simulated reflection phases as the consequence of l ranging from 1.5 to 1.8 mm (l denotes the period of EBG). As seen, when the period of EBG cell gets larger, resonant frequency moves toward lower bands. According to Eqs. (2) and (3) in [11]: $L = (\mu_0 D/2\pi)\ln(2D/\pi t)$, $C = ((d(\varepsilon_r + 1)\varepsilon_0)/\pi)\ln(2D/\pi\delta)$. Where D indicates the grid size of UC-EBG, δ indicates the strip width, ε_0 indicates vacuum dielectric constant, t and d indicate part widths of UC-EBG, respectively. Some equivalent relations exist between UC-EBG in

Please cite this article in press as: N. Wang, et al. Bandwidth and gain enhancement of optically transparent 60-GHz CPW-fed antenna by using BSIS-UC-EBG structure, Photon Nanostruct: Fundam Appl (2014), http://dx.doi.org/10.1016/j.photonics.2014.11.002

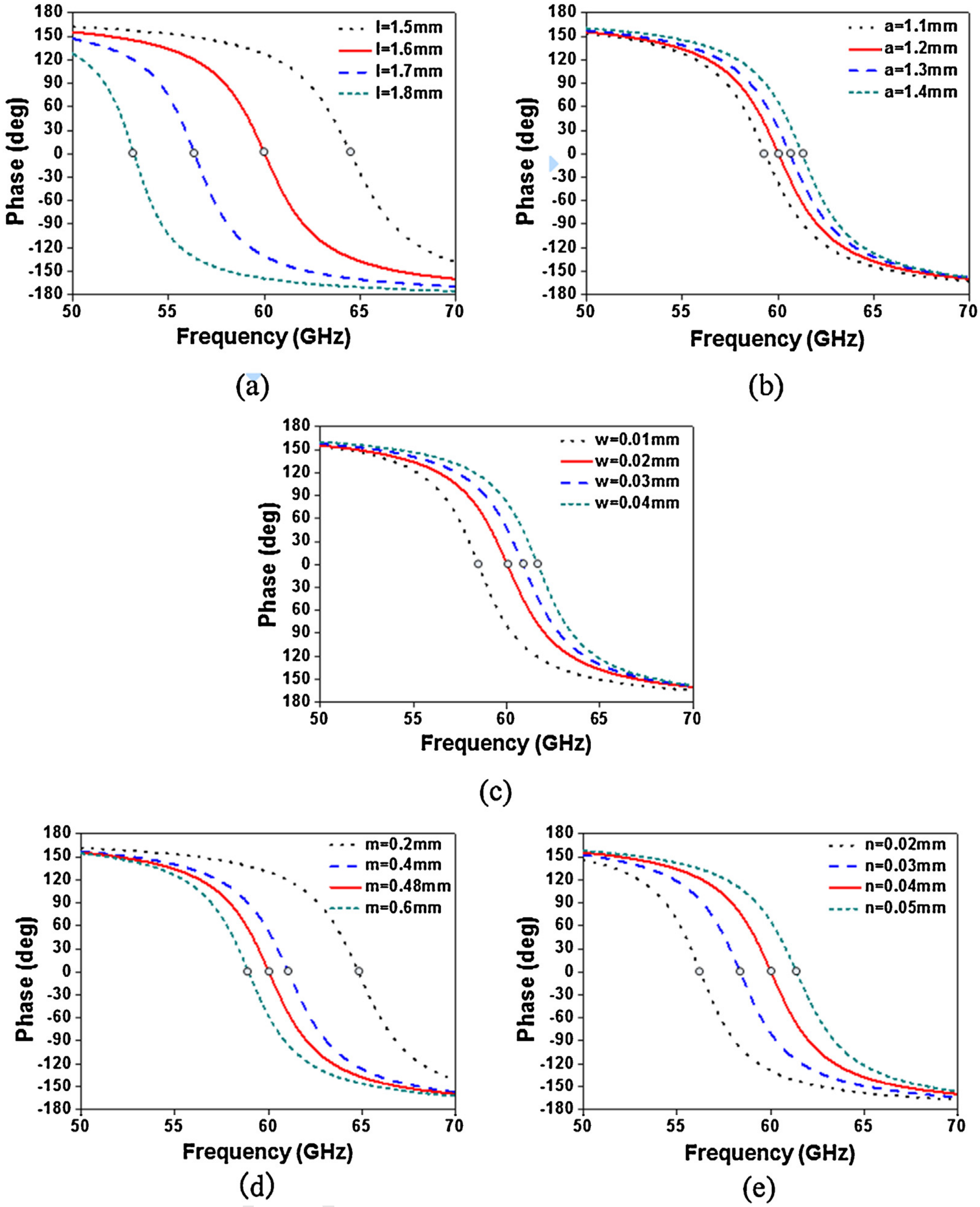

Fig. 5. Simulated reflection phase as a function of (a) l, (b) a, (c) w, (d) m, (e) n.

[11] and BSIS-UC-EBG in this paper, which is shown as follows: $l = D$, $w = \delta$, $a = D - t$. Where grid inductance L and conductance C increase as the grid periodical size l increases, so resonant frequency, which can be calculated by $f_r = 1/(2\pi\sqrt{LC})$, will decrease correspondingly. Apparently, the most applicable reflection phase characteristic can be acquired when $l = 1.6$ mm. In a similar way, the width (w) of strip which forms electrical inductance can have a reverse effect on C, thus resonant frequency will be higher along with larger width, as shown in Fig. 5(c). The red curved line of $w = 0.02$ mm is selected to be the accurate size of the strip. Due to formulas mentioned above, the process that a affects the resonant frequency can be elaborated as follows: when a varies from 1.1 to 1.4 mm (other parameters are fixed at the same time), t becomes smaller. Therefore L gets smaller, which make the phase curve shifts to right (Fig. 5(b)).

Please cite this article in press as: N. Wang, et al. Bandwidth and gain enhancement of optically transparent 60-GHz CPW-fed antenna by using BSIS-UC-EBG structure, Photon Nanostruct: Fundam Appl (2014), http://dx.doi.org/10.1016/j.photonics.2014.11.002

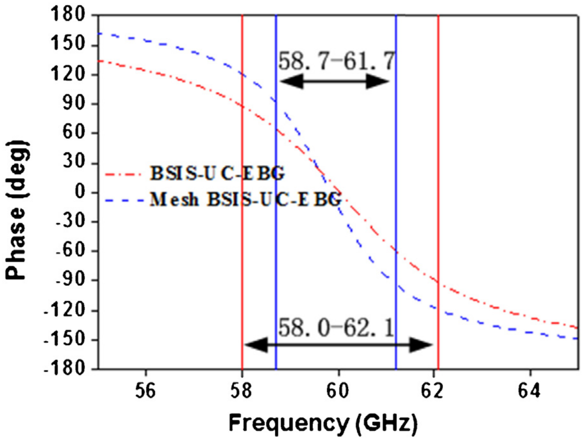

Fig. 6. Comparison of reflection phase curves for BSIS-UC-EBG and mesh BSIS-UC-EBG.

Curve movements over different m and n can be analyzed in a different manner (Fig. 5(d) and (e)). Equivalent relations like $C=\varepsilon\varepsilon_0 S/n$, $C=\varepsilon S/4\pi kd$, $m=D-2\times t-d$ are used for our analysis. When m gets larger (D and t are fixed), d gets smaller, which leads to a larger C and a smaller f_r. Just as shown in Fig. 5(d), resonant frequency gets lower along with a larger m. The $m=0.48$ mm, which obtains resonant frequency at 60 GHz, is chosen to be the final size. Similarly, an increase of n will lead smaller C, therefore resonant frequency has the same tendency with n. And $n=0.04$ mm is selected. Sizes shown in Table 1 are chosen to obtain the best performance for 60 GHz BSIS-UC-EBG and mesh BSIS-UC-EBG.

Based on the BSIS-UC-EBG, the mesh BSIS-UC-EBG is also simulated in the same way as shown in Fig. 4. The mesh structure induces self-inductors and other capacitances. The self-inductor of half grid can be calculated by series–parallel formulas of inductance and capacitance:

$$L_s \approx \frac{17L_0}{6} \qquad (4)$$

L_0 is the inductance of the 0.01 mm width, 0.2 mm long trip, and be calculated by [25]

$$L_0 = \frac{\mu_0 l_i}{2\pi}\left[\log\frac{2l_i}{w}+\frac{1}{2}\right] \qquad (5)$$

where $l_i=0.2$ mm, $w=0.01$ mm. Thus the equivalent inductance of the mesh grid has increased. According to $C=((d(\varepsilon_r+1)\varepsilon_0)/\pi)\ln(2D/\pi\delta)$, the capacitance of the grid has decreased because of the decrease of permittivity, which offsets the influence of inductance on resonant frequency. The reflection phase curve is plotted in Fig. 6. Property comparisons of two EBGs have been displayed. It is obvious that center frequencies of both structures are around 60 GHz. Frequency band-gap, defined as reflection phase between ±90°, lies at 58.7–61.7 GHz for mesh BSIS-UC-EBG, which is slightly narrower than the 58.0–62.1 GHz band of transparent BSIS-UC-EBG.

3.2. *Results comparisons of the two kinds of optically transparent antennas*

Comparisons on reflection coefficients of antennas have been shown in Fig. 7. As seen, impedance bandwidth of transparent antenna lies between 55.5 and −68 GHz (20.2%) with its center frequency at 61.75 GHz. When the BSIS-UC-EBG periodic structure has been placed around the radiating patch, a larger bandwidth of 36.6% centered at 60.35 GHz (49.3–71.4 GHz) is obtained (depicted by the curve of transparent BSIS-UC-EBG antenna), which is shown in Fig. 7(a). By that

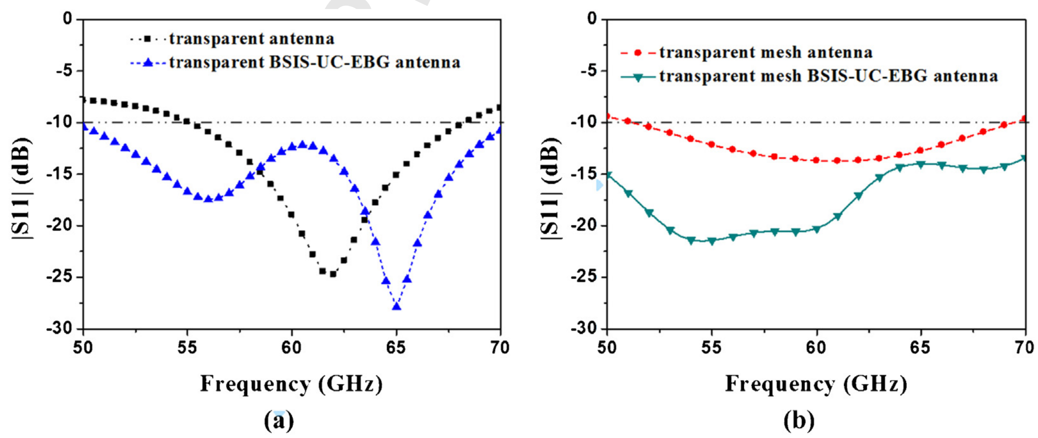

Fig. 7. Comparisons of reflection coefficients among (a) transparent antenna and transparent BSIS-UC-EBG antenna; (b) transparent mesh antenna and transparent mesh BSIS-UC-EBG antenna.

Please cite this article in press as: N. Wang, et al. Bandwidth and gain enhancement of optically transparent 60-GHz CPW-fed antenna by using BSIS-UC-EBG structure, Photon Nanostruct: Fundam Appl (2014), http://dx.doi.org/10.1016/j.photonics.2014.11.002

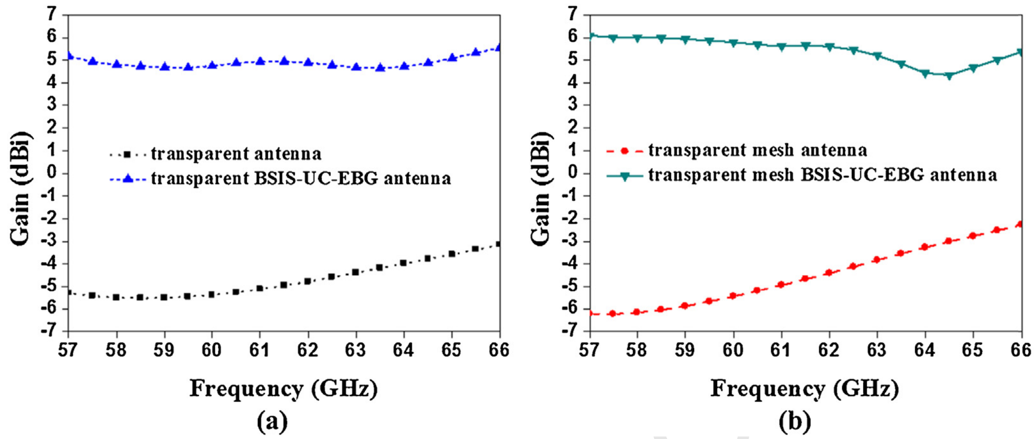

Fig. 8. Comparisons of gains among (a) transparent antenna and transparent BSIS-UC-EBG antenna; (b) transparent mesh antenna and transparent mesh BSIS-UC-EBG antenna.

analogy, transparent mesh BSIS-UC-EBG antenna has a bandwidth of 46–72.5 GHz (44.7%), which is 8.3 GHz wider than transparent mesh antenna (Fig. 7(b)). It can be concluded from Fig. 7 that two advantages have been introduced by BSIS-UC-EBG: one is that a larger impedance bandwidth can be obtained, and the other is that the resonant frequency can be closer to 60 GHz. Meanwhile, compared the two curves of antennas with different EBGs, a conclusion can be drawn that transparent mesh BSIS-UC-EBG antenna has a wider bandwidth than transparent BSIS-UC-EBG antenna.

Fig. 8 illustrates gain performances for four antennas. Fig. 8(a) shows that transparent BSIS-UC-EBG antenna has a gain of 4.7 dBi (10 dBi higher than transparent antenna at 60 GHz), which is stable at around 5 dBi during the unlicensed band. Antenna gain has been dramatically improved by EBG structure. In Fig. 8(b), remarkable gain enhancement of 11.23 dBi is also obtained by transparent mesh BSIS-UC-EBG antenna compared with transparent mesh antenna. Thus, it is worth mentioning that the third advantage brought by BSIS-UC-EBG is prominent gain enhancement, which

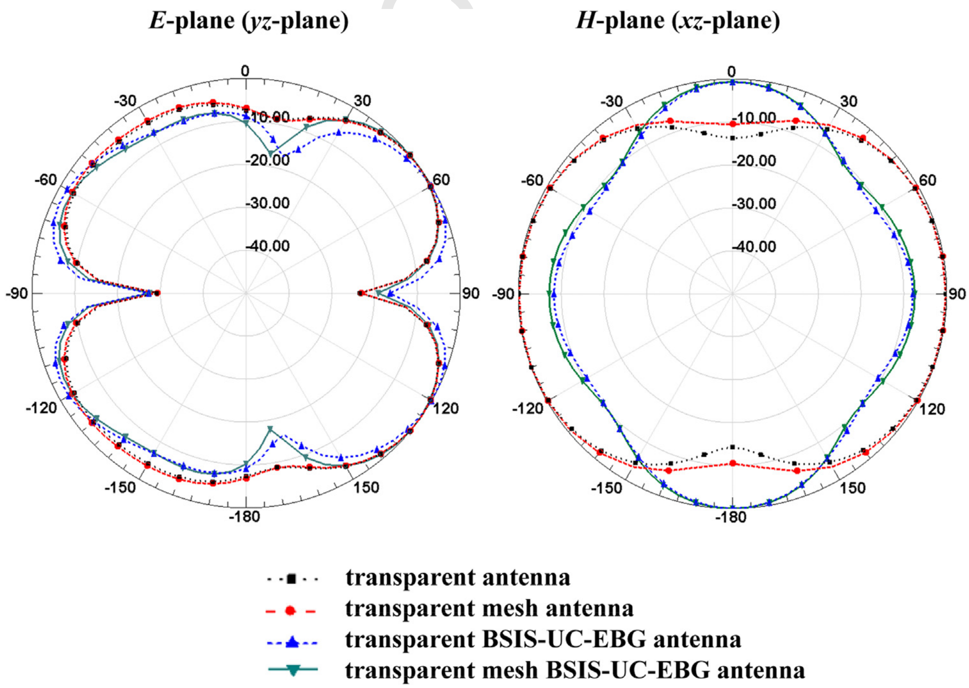

Fig. 9. Comparison of radiation patterns between antennas at 60 GHz.

Please cite this article in press as: N. Wang, et al. Bandwidth and gain enhancement of optically transparent 60-GHz CPW-fed antenna by using BSIS-UC-EBG structure, Photon Nanostruct: Fundam Appl (2014), http://dx.doi.org/10.1016/j.photonics.2014.11.002

has great significance for design of high gain and wideband antennas. As an optically transparent antenna features good performances over impedance bandwidth and gain, transparent mesh BSIS-UC-EBG antenna is suitable for many millimeter wave applications which have special requirements for transparency, security or esthetics. Besides, a higher average gain is obtained by mesh BSIS-UC-EBG antenna than BSIS-UC-EBG antenna. It can prove that better transparency has no bad effect on antenna performances.

As antennas are printed on the *xy*-plane and each monopole is in the *y*-direction, the *E*-plane and *H*-plane for the antennas are the *yz*-plane and *xz*-plane, respectively. The radiation patterns of four antennas at 60 GHz are depicted in Fig. 9. It can be seen that radiation patterns in *E*-plane and *H*-plane are basically the same. Little effect has been caused by the mesh-introduced process and the BSIS-UC-EBG. The characteristic depicted by Fig. 9 is similar to that of the half wave dipole antenna, whose *H*-plane radiation is omni-directional.

4. Conclusions

In summary, we presented a novel bidirectional symmetric I-shaped slot uniplanar compact electromagnetic band-gap (BSIS-UC-EBG) structure. The reflection phase band of 58.0–62.1 GHz of this new EBG was obtained. Both transparent BSIS-UC-EBG antenna and transparent mesh BSIS-UC-EBG antenna based on the BSIS-UC-EBG were proposed to achieve properties of wideband, high gain and transparency. Those two high performance antennas were designed on a 0.2 mm-thick 7980 Corning substrate. The analysis results display that: (1) Compared with transparent antenna without BSIS-UC-EBG, 9.6 GHz bandwidth enhancement and 10 dBi gain improvement of the transparent BSIS-UC-EBG antenna can be achieved. (2) Compared with transparent mesh antenna without BSIS-UC-EBG, 8.3 GHz bandwidth enhancement and 11.23 dBi gain improvement of the transparent mesh BSIS-UC-EBG antenna can be achieved. Particularly, compared with the transparent BSIS-UC-EBG antenna, the transparent mesh BSIS-UC-EBG antenna can effectively enhance the antenna transparency without decreasing the antenna property. Thus, the comparison results confirm that the designed BSIS-UC-EBG and mesh BSIS-UC-EBG can dramatically improve the antenna's properties of gain and bandwidth. It is potentially an ideal transparency components used for wireless communications.

Acknowledgments

This work was supported in part by the NSFC under Grant No. 61372038, the NSFC under Grant No. 61431003, the National 973 Program under Grant No. 2012CB315705, and the Fund of the State Key Laboratory of Information Photonics and Optical Communications (Beijing University of Posts and Telecommunications), China.

Q5 Q6

References

[1] R.N. Simons, R.Q. Lee, Feasibility study of optically transparent microstrip patch antenna IEEE AP-S Int. Symp. Dig., Montreal, QC, Canada, vol. 4, 1997, pp. 2100–2103.

[2] C. Mias, C. Tsakonas, N. Prountzos, Optically transparent microstrip antennas, in: IEE Colloquium on Antennas for Automotives (Ref. No. 2000/002), London, England, 2000, pp. 8/1–8/6.

[3] F. Colombel, X. Castel, M. Himdi, G. Legeay, S. Vigneron, E.M. Cruz, Ultrathin metal layer, ITO film and ITO/Cu/ITO multilayer towards transparent antenna, IET Sci. Meas. Technol. 3 (2009) 229–234.

[4] N. Guan, H. Furuya, K. Himeno, K. Goto, K. Ito, A monopole antenna made of a transparent conductive film, in: IWAT'07, Cambridge, USA, 2007, pp. 263–266.

[5] A. Katsounaros, Y. Hao, N. Collings, W.A. Crossland, Optically transparent antenna for ultra wide-band applications, in: Proc. Eur. Conf. Antennas Propag., Berlin, Germany, 2009, pp. 1918–1921.

[6] J. Hautcoeur, F. Colombel, X. Castel, M. Himdi, E. Motta Cruz, Optically transparent monopole antenna with high radiation efficiency manufactured with silver grid layer (AgGL), Electron. Lett. 45 (2009) 1014–1016.

[7] J. Hautcoeur, F. Colombel, M. Himdi, X. Castel, Large and optically transparent multilayer for broadband H-Shaped slot antenna, LAWP 12 (2013) 933–936.

[8] J. Hautcoeur, L. Talbi, K. Hettak, Feasibility study of optically transparent CPW-fed monopole antenna at 60-GHz ISM bands, IEEE Trans. Antennas Propag. 61 (2013) 1651–1657.

[9] Z. Guo, H. Tian, X. Wang, et al., Wide-bandwidth, high-gain, low-temperature cofired ceramic magneto-electric dipole antenna and arrays for millimeter wave radio-over-fiber systems, Photonics Res. 2 (2014) B40–B44.

[10] J.C. Iriarte, A. Tellechea, I. Ederra, R. Gonzalo, EBG Antenna Technology for Different Applications, ICEAA, Torino, Italy, 2013, pp. 884–886.

[11] D.N. Elsheakh, H.A. Elsadek, E.A. Abdallah, H. Elhenawy, M.F. Iskander, Enhancement of microstrip monopole antenna bandwidth by using EBG structures, LAWP 8 (2009) 959–962.

[12] S. Chauhan, P.K. Singhal, Design of UWB monopole antenna with EBG structure and ground with rectangular slots, Int. J. Emerg. Trends Sci. Technol. 01 (2014) 572–575.

[13] A. Kumar, D. Arya, D.K. Srivastava, Band Width of Microstrip Antenna Improved by Using Mushroom Type EBG Structure, IMPACT, Aligarh, India, 2013, pp. 159–162.

[14] A. Kumar, V.D. Kumar, M.P. Abegaonkar, S.K. Koul, A Microstrip Patch Antenna with Metamaterial and EBG Structures, ICSC, Noida, India, 2013, pp. 27–32.

[15] A.E.I. Lamminen, J. Saily, A.R. Vimpari, 60-GHz patch antennas and arrays on LTCC with embedded-cavity substrates, IEEE Trans. Antennas Propag. 56 (2008) 2865–2874.
[16] A.E.I. Lamminen, A.R. Vimpari, JussiSäily, UC-EBG on LTCC for 60-GHz frequency band antenna applications, IEEE Trans. Antennas Propag. 57 (2009) 2904–2912.
[17] N. Ma, H. Zhao, Reduction of the Mutual Coupling Between Aperture Coupled Microstrip Patch Antennas Using EBG Structure, IWS, X'ian, China, 2014, pp. 1–4.
[18] S. Ebadi, A. Semnani, Mutual coupling reduction in waveguide-slot-array antennas using electromagnetic bandgap (EBG) structures, IEEE Antennas Propag. Mag. 56 (2014) 68–79.
[19] L. Matekovits, Y. Ranga, Controlling the phase of the scattered and/or radiated field from a high impedance surface of quasi-periodic sequences, IEEE Antennas Wirel. Propag. Lett. 12 (2013) 321–324.
[20] M. Hosseini, D.M. Klymyshyn, G. Wells, X. Liu, Thick metal EBG cells with narrow gaps and application to the design of miniaturized antennas, Prog. Electromagn. Res. 145 (2014) 185–193.
[21] W.E. McKinzie II, D.M. Nair, B.A. Thrasher, M.A. Smith, E.D. Hughes, J.M. Parisi, 60 GHz Patch Antenna in LTCC with an Integrated EBG Structure for Antenna Pattern Improvements, APSURSI, Memphis, USA, 2014, pp. 1766–1767.
[22] A. Tellechea, J.C. Iriarte, I. Ederra, R. Gonzalo, Dual Band Compact and Light EBG Superstrate Based Antenna for TT &C Applications, EuCAP, Gothenburg, Sweden, 2013, pp. 2505–2507.
[23] Y. Ranga, L. Matekovits, A.R. Weily, K.P. Esselle, A low-profile dual-layer ultra-wideband frequency selective surface reflector, Microw. Opt. Technol. Lett. 55 (2013) 1223–1227.
[24] Y. Ranga, L. Matekovits, K.P. Esselle, A.R. Weily, Multi-octave frequency selective surface reflector for ultrawideband antennas, IEEE Antennas Wirel. Propag. Lett. 10 (2011) 219–222.
[25] C.R. Sochava, High-impedance surfaces based on self-resonant grids, Analytical modelling and numerical simulations, Prog. Electromagn. Res. 43 (2003) 239–256.

Please cite this article in press as: N. Wang, et al. Bandwidth and gain enhancement of optically transparent 60-GHz CPW-fed antenna by using BSIS-UC-EBG structure, Photon Nanostruct: Fundam Appl (2014), http://dx.doi.org/10.1016/j.photonics.2014.11.002